

Modelling and an adaptive fuzzy logic controller of solar thermal power plant

Abstract. This article aims to model and control a solar thermal power plant. The modeling and the dynamic behavior of the system have been well studied and carried out the variation of the exchanger temperature by acting on different parameters, such as the length, the exchange surface, and the exchange coefficient. A comparison was made between conventional PI control and an advanced AFLC-PI fuzzy logic-based control to drive the steam turbine. This advanced command improves the system's robustness with respect to internal disturbances (parametric variations) and external disturbances (sudden pressure variations).

Streszczenie. Celem artykułu jest modelowanie i sterowanie elektrownią słoneczną. Modelowanie i dynamiczne zachowanie systemu zostały dobrze zbadane i przeprowadzono zmianę temperatury wymiennika poprzez oddziaływanie na różne parametry, takie jak długość, powierzchnia wymiany i współczynnik wymiany. Dokonano porównania między konwencjonalnym sterowaniem PI a zaawansowanym sterowaniem opartym na logice rozmytej AFLC-PI do napędzania turbiny parowej. To zaawansowane polecenie poprawia odporność systemu na zakłócenia wewnętrzne (zmiany parametryczne) i zewnętrzne (nagłe zmiany ciśnienia) (**Modelowanie i adaptacyjny regulator logiki rozmytej elektrowni słonecznej**)

Keywords: Parabolic cylinder collectors, solarenergy, steam generator, thermo-solar power station, turbine, PI, fuzzy controller.

Słowa kluczowe: Kolektory paraboliczne cylindryczne, energia słoneczna, generator pary, elektrownia termo-słoneczna, turbina, Regulator PI ozmyty kontroler.

1. Introduction

The production of electrical energy by power plants using fossil fuels remains the primary problem researchers are battling to overcome [1]. According to the British weather service, which mentions a risk of temperature rise that will reach +1.5 °C by 2024, this is the highest value it has not previously registered [2]. So far, all countries use fossil fuels in all sectors, as shown in figure 1.

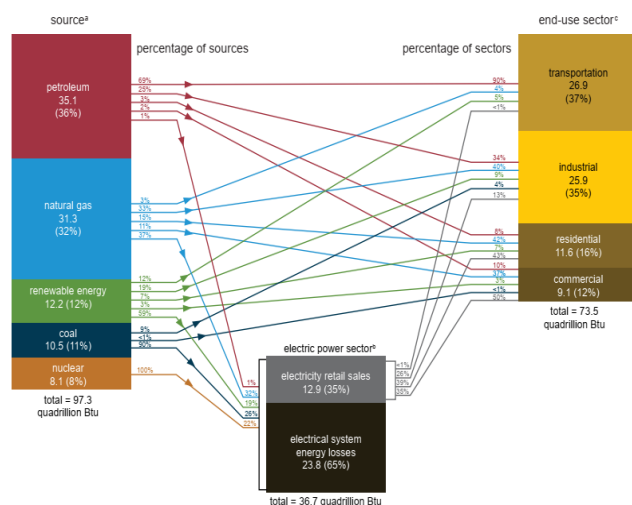


Fig.1. World primary energy consumption by source and sector, 2021 [3]

Greenhouse gas (GHG) emissions are linked to this energy. According to Figure 1, in 2020, primary energy (oil, coal, and natural gas) will precede all other fuels at the global level. Also, we see that oil dominates further energy because it is a lucrative source. Since the 1950s, it has satisfied more than 30% of energy needs as it is the primary raw material for fuels that supply transport (cars, trucks, planes, ...etc.).

According to the World Meteorological Organization (WMO), roughly half of the carbon dioxide (CO₂) emitted by human activities today remains in the atmosphere. The rest is absorbed by the oceans and terrestrial ecosystems [4].

Energy-related emissions depend on the level of energy consumption as well as on the primary energy mix, which

globally remains dominated by fossil fuels in 2018, according to Figure 1 (oil, coal, and natural gas). Each year, 37 gigatons of CO₂ are released into the atmosphere, mainly by human activities (combustion of fossil fuels, deforestation, etc.).

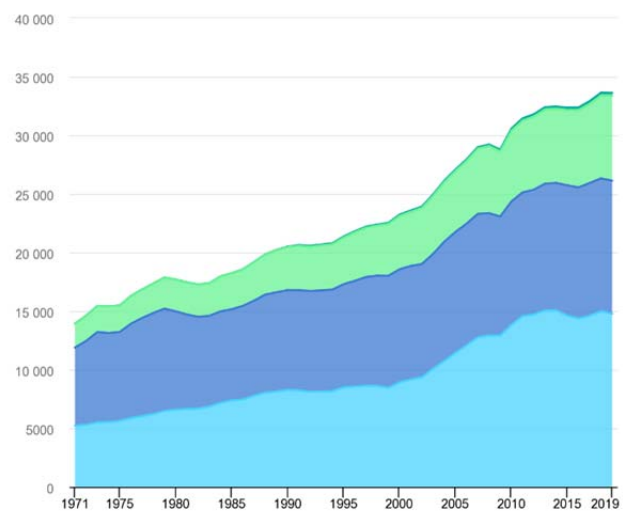


Fig.2. World CO₂ emissions from fuel combustion by fuel, 1971-2019 [5]

The consequences of such a situation will lead to the following results:

- The polar regions are losing ice between 2006 and 2015. The mass of the Greenland ice sheet decreased by 278 ± 11 gigatons per year (Gt/year). These losses have contributed to the global rise in the sea level of 0.77 ± 0.03 and 0.43 ± 0.05 mm/year. This elevation leads to:

- Flooding Rise in sea level, hence the disappearance of coastal towns.
- Deforestation
- Oxygen pollution
- Drought.

To avoid or minimize these dangers, we use renewable energy. An energy source is said to be renewable if the fact

of consuming it does not limit its future use; this is the case with energy from the sun, wind, rivers, biomass ... etc. Renewable energies, therefore, constitute an alternative to fossil fuels in several ways.

- They generally disturb the environment less.
- do not emit greenhouse gases and do not produce waste.
- They are inexhaustible.
- They allow decentralized production.

The evolution of solar system technology has made it possible to have two forms of solar energy sources:

- Solar photovoltaic: a solar system made up of photovoltaic cells directly converts part of the solar radiation into electricity by the photovoltaic effect [6]. The application of this technology can be found in several fields, such as lighting, watches, door control, traffic signs, etc. [6].
- Solar thermal: the use of solar energy to produce heat by heating a fluid to a higher or lower temperature. If the temperature of the fluid is high enough, then a thermodynamic cycle can be used to generate electricity and heat; this is the field of thermodynamic power plants [7]. We find this application in several fields: solar furnaces, solar water heaters and solar thermal power plants ... etc.

The objective of this paper is to improve the dynamic response of the steam turbine of a thermal power plant by applying conventional and advanced regulators. This study elaborates on using several PID control schemes to achieve efficiency and distinguishes the performance of each system. It also demonstrates how a change in the controller can affect efficiency. A great deal of previous research in this field has focused on the control schemes, like Murshitha Shajahan et al. in [8] brief on some of the most effective control configurations that can be used to improve the efficiency of the thermal power plant. Also, Alobaid et al. [9] comprehensively review dynamic simulation, its development, and its application to various thermal power plants. In [10], Al-Maliki et al. describe the advanced controllers used in the thermal power plant. In [11], Cao et al. propose an adaptive neuro-fuzzy inference system-based pulverizing capability model (ANFIS-PCM) to control thermal power plants. Furthermore, Liao et al. [12] present a cooperative distributed model predictive control (C-DMPC) strategy for load frequency control for solar thermal power plants, and Terunuma et al. [13] propose a predictive model controller for solar thermal power plants.

This paper has been divided into four parts.

The second part deals with modelling some components of the thermo-solar system, including the solar collector, the steam generator, the over-valve, and the turbine.

The third part is devoted to classic control by a PI regulator.

In the fourth part, we will synthesize and apply a fuzzy regulator for the dynamics of the turbine. Finally, we will present and interpret the results of the simulation.

II. Solar thermal power plant Description and functioning.

This type of plant is based on alignments of curved mirrors which concentrate the solar rays onto a receiving tube located along the reflector's focal line. In this tube circulates, a heat transfer fluid that goes to a steam generator will yield its thermal energy to a second circuit containing a second motive fluid. The motive fluid expands in the turbine to create a mechanical torque [14], [15].

II.1. Sensor.

They are solar collectors based on direct solar radiation and focus it on the absorber tube, the latter allowing high temperatures of between 400 °C and 1000 °C to be reached. This type of sensor is used in steam plants to

vaporize water [16]. There are several types of concentration sensors.

A detailed study of these sensors, such as the material, the number of panes, the distance between panes and the nature of the absorbing layer of the deflector gave the following results [17]:

- In the absence of glass, the sensor heats up, and the efficiency of a sensor drops rapidly.
- For the exact distance between panes (15 mm), the efficiency obtained for three panes remains lower than that obtained with one or two panes. Beyond the two windows, the heating is more prolonged, and thermal losses prevail. For this, the use of two windows in the refrigeration remains better.
- Plastic and copper remain better for the materials used (plastic, silver, stainless steel, aluminium, plastic and copper).

On the other hand, the absorber must be designed in such a way as to maximize the thermal absorption of the radiation while limiting the thermal losses. Thus, the requirement for surface coating and the refinement of the air layers between the successive panes also help to limit convective losses. In the new techniques, these losses are reduced by using tubular absorbers for excellent control of the collection, which is the optimal goal of the absorbers [18]).

The choice of fluid is, therefore, necessary. However, the fluid must be chosen to meet the most important criteria (impact on the environment, ease of supply, and lowest possible cost). Among the fluids used are oil, water, and melted salts, which have different characteristics [19].

These salts are solid at room temperature. To use them as a fluid, they must be maintained at a minimum temperature of around 270 °C.

Finally, thermal water and oils are the fluids most widely used in power plants. The water used as a heat transfer fluid shows its limits at low temperatures. So, in this case, the presence of a heat-producing steam exchanger-evaporator becomes necessary. Oils also have their temperature limits. The risk of pollution also leads to the elimination of the use of thermal oils.

After studying the different fluids and their fields of use, we are interested in the different solar collectors.

➤ The different solar collectors

- **Parabolic cylinder manifolds (CCP):** It is the most proven technology (74% of thermodynamic solar installations use it). The reflectors follow the sun's path and concentrate the solar flux onto horizontal tubes attached to the receivers. A heat-transferring fluid circulates in the tubes at temperatures between 270 and 450 °C [20].
- **Heliostats and concentration towers:** Heliostats are reflectors with a two-axis sun tracking system. The solar rays are then concentrated at the top of a fixed tower (15% of thermodynamic solar systems). The temperature in the absorber can reach, at the top of the tower, 450 to 1000 °C [21].
- **Parabolic mirrors:** These mirrors follow the sun's course along two axes and concentrate the solar flux into a focal point (2% of thermodynamic solar systems). The temperatures attainable at heart are of the order of 600 to 1200 °C [20].

II.2. Exchanger.

The fluid leaving the sensor goes to the heat exchanger, which is influenced by several parameters, which are [22]:

- The size of the exchanger: an exchanger with thicker walls containing more liquid has a greater time constant than a second exchanger with thinner walls.

- The fluid flow rate F : It can be seen that whatever the geometry of the exchanger, the time constant increases very rapidly in laminar flow when the mass flow rate decreases. At the same time, it varies very little in a turbulent flow.

II.3. The servo valve.

Servo valves constitute the top of the range of proportional action distributors. The nozzle-pallet stage controls the movement of the drawer. The pallet is integral to the mobile armature of a torque motor, the displacement of which is proportional to the control current. The distributor drawer is slaved in the position either with electrical feedback, mechanical feedback, or barometric feedback, as shown in figure 3 [23].

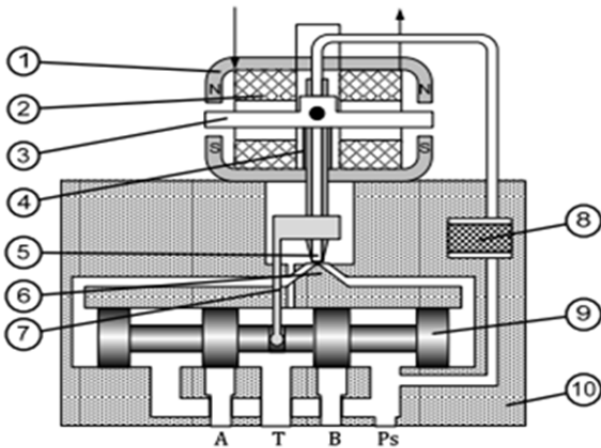


Fig.3. Internal view of a servo valve.

- 1- Torque motor.; 2- Magnet and coil.; 3- Mobile armature.; 4- Fixed metal tube.; 5- Nozzle.; 6- Receiver port.; 7- Feedback spring.; 8- Filtered.; 9- Dispensing drawer.; 10- Valve body.

We can say that the servo valve is a progressive solenoid valve whose flow depends on the control current. They are characterized by their high static (precision, hysteresis, etc.) and dynamic performances, but also by their higher acquisition and maintenance costs. The pressure of the steam leaving the exchanger is regulated by a servo valve specially designed for applications in gas and steam turbines [24].

II.4. The turbine.

The turbine's HP, MP, and LP stages contain a series of blades arranged around a wheel integral with the shaft. The steam deflected by these vanes thus creates a powerful mechanical torque. The blades are particularly hard steel to withstand high temperatures and intense centrifugal forces [25].

Among the problems to be addressed in the operation of steam turbines are, for example, humidity and condensation in forms (liquid film, large drops). These droplets then enlarge during the expansion to form a liquid film streaming on the internal wall of the turbine. Humidity is the cause of 25% of the loss of efficiency.

The fluid in its path is controlled by valves which will experience oscillating load and high-frequency disturbances, so the presence of static friction in the control valve is the most common reason. Control valves can have oscillatory behavior, affecting control performance and increasing the control loop's variability [26].

When the fluid reaches the turbine, the fluid expands to generate an engine torque which drives a generator.

III. Modeling and characteristics of the system.

Figure 6 shows the operation of the solar thermal system where the solar collectors reflect the solar flux on the absorber, which contains the heat transfer fluid. This fluid, being brought to high temperature, goes to the steam generator, where thermal energy is exchanged with the driving fluid. This pressurized fluid will expand in the turbine to produce mechanical energy capable of driving the synchronous generator. Servo valves are used to control the flow to control the speed.

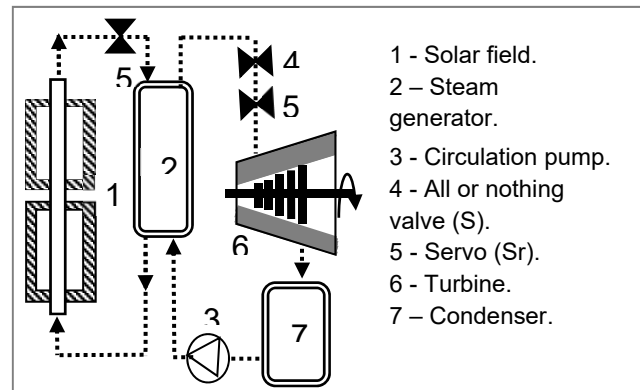


Fig.4. Components of a solar thermal power plant

III.1. Sensor modeling.

Parabolic collectors are made by folding a sheet of reflective material into a parabolic shape. A black metal pipe, covered with a glass tube to reduce heat loss, is placed along the focal line of the collector. The concentrated radiation reaches the receiving tube and heats the fluid flowing through the tube. It thus transforms solar radiation into proper heat. The three-dimensional view of a parabolic cylinder sensor is shown in figure 5.

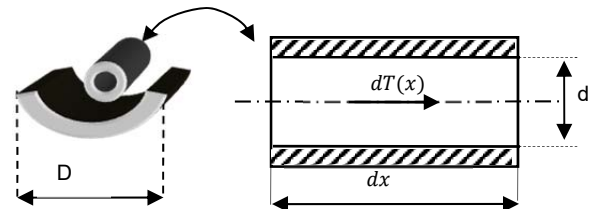


Fig.5. Parabolic cylinder sensor

The parabolic cylinder sensor is governed by equation 1 [27].

$$(1) \quad dx = \frac{dT_f(x)}{\frac{1}{m \cdot c_p} [S \cdot D \cdot \rho \cdot \gamma \cdot \alpha - K(T_f - T_a)] \cdot \pi \cdot d}$$

Where:

S : Solar flux considered constant= 700W/m^2 ; D : Cylinder opening diameter = 2.5m ; ρ : Reflectivity = 0.86 (without unit); λ : Reflected solar flux fraction= 77% ; α : Absorption coefficient= 0.94 (it's a black tube); k : Global exchange coefficient= $7\text{W/m}^2 \cdot \text{K}$; d : Tube diameter= 6cm .

III.2. Modeling of the exchanger

A heat exchanger is a device for transferring heat from a source to a heat sink. this exchange can be done through a solid wall without mixing fluid or by mixing two fluids [28].

The exchanger is the most important part of the plant. Its construction is a bit tricky. It is checked in case of a leak (crack in a tube for example) by one of the following two methods:

- If the crack is located in an accessible location, the search is carried out by NDC control (non-destructive control), which is based on the use of three successive products:
 - The cleaner or degreaser with which we rinse the place where the crack is located.
 - The penetrator: a red product which must be placed on the cleaned part.
 - The developer: a white product which covers the same part. The red colour disappears except for the trace of the crack, which remains with evident limits.
- If the crack is not accessible, we use the boroscope, a small remote-controlled camera connected to a PC. A simplified diagram of the shell and tube exchanger is shown in figure 6.

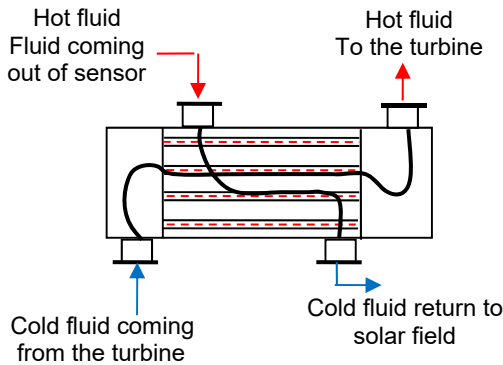


Fig.6. Tube heat exchanger

The exchanger is governed by equation 2 [28].

$$(2) \quad T_2 = T_{2s} - z \cdot \frac{T_{1e} - T_{2s}}{1-z} \left[1 - \exp \left[-k \cdot \left[\frac{1}{m_1 \cdot c_{p1}} - \frac{1}{m_2 \cdot c_{p2}} \right] \cdot S \right] \right]$$

Where:

T_{e1}, T_{s1} : Primary circuit inlet outlet temperature. [°C]

T_{e2}, T_{s2} : Second circuit inlet outlet Temperature. [°C]

Z: Heat capacity report.

S: Fluid passage section. [m²]

m_1, m_2 : Mass flow of the two fluids [kg/s].

C_{p1}, C_{p2} : Specific heat of the two fluids [J/kg.k].

III.3. Modeling of the servo valve.

The steam passes through the pipes to the valve bodies flanged on the turbine. Each valve body comprises an isolation valve (all or nothing: AON) denoted S and a control valve denoted Sr (servo valve). The isolation valve is located upstream of the control valve (Fig. 4).

The following transfer function characterizes the dynamics of a servo valve.

$$(3) \quad F(p) = \frac{k}{1+2\xi\tau_n p + \tau_n^2 p^2}$$

K : static gain of the servovalve.

ξ = damping coefficient related to construction

$\tau = \frac{1}{\omega_0}$ (Proper pulsation given by the constructor)

III.4. Modeling of the turbine.

It is considered that the fraction of the mechanical power developed by each stage is proportional to the vapor flow rate at the outlet of this stage.

The pressure entering the stage (HP) is proportional to the opening section of the control valve (s) and the amount of pressure exiting the superheater.

When the flow rate at the inlet of the turbine changes, it will automatically change at the outlet of the stage (HP) and

become dHP with a specific time constant THP (around 0.1 to 0.4s).

We obtain such a transfer function by expressing proportionality between the outgoing flow and the pressure prevailing at the same stage, as shown in figure 7.

We denote by FHP the fraction of mechanical power delivered by the stage (HP), which is 30% of the total power delivered by the turbine. The pressure will take 4–11 s to get out of the superheater; it is a bit of a long journey.

S1: Represents the passage section in the valves interception.

F_{MP} and F_{BP}: Represent the total power fractions delivered respectively by the stages (MP) and (LP), it sounds in the range of 40% and 30%.

The time constant in the stage (LP) is analogous to that of (HP), it is (of the order of 0.3 to 0.5s) [10].

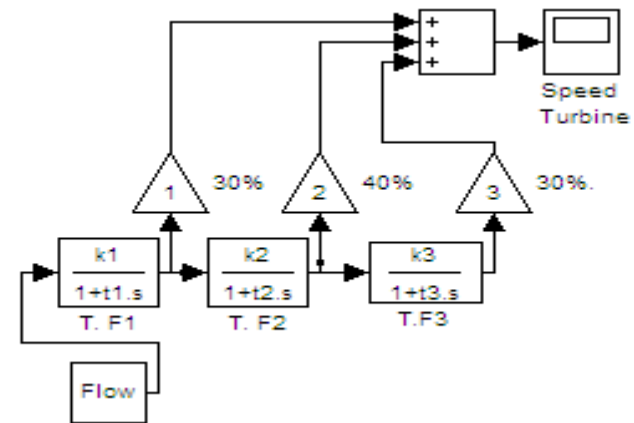


Fig.7. The turbine blocks

IV. Turbine control.

For the network frequency to be stable, the alternator must run at a constant speed, and since the alternator is coupled with the turbine, we have to control the turbine.

IV.1. PI regulator.

PI regulator: In most industrial processes, particularly in rotating machines, it is essential to control specific physical parameters (speed, position, etc.). It is often necessary to use a control. The Proportional Integral (PI) control is a proven method that gives good results thanks to the proportional action, which improves the speed and the integral and cancels the static error.

There is no strict rule for the choice of a corrector; however, we can indicate some general considerations that derive from the properties of current correctors.

- Series correction: the most widely used method of synthesizing controlled systems.
- PI regulator: the most used because of:
 - It's very good static precision, the integral term ensuring a zero static deviation.
 - Good speed if the parameters are well adjusted.

In addition to that the PI regulator is physically feasible.

It is modeled by the following transfer function:

$$(4) \quad H = k \left(1 + \frac{1}{T_i \cdot s} \right)$$

To find the regulator gains, we apply the Ziegler-Nichols method. In this method (figure 8), it is not necessary to know the detailed structure of the system. We note, experimentally, its open-loop response.

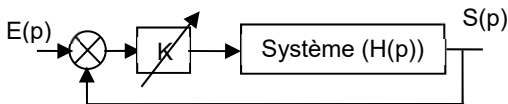


Fig.8.Ziegler-nichols method

When modifying the gain G , we will have the oscillation of the signal S , and then we note the critical values, the period T_c and the gain G_c . The obtained results are:

$G_c=9.55 - T_c=6.5s$

Regulator type	K_p	K_i
PI	5.73	0.56

To analyze the dynamics of our closed loop system, a speed reference value of 3000 tr/min is applied to the input of the turbine.

IV.2. Fuzzy logic controller:

Used to represent uncertain and imprecise knowledge. Moreover, it is used to make decisions even if the inputs and outputs can only be estimated from vague predicates.

It can control nonlinear, uncertain, and adaptive systems, giving robust parameter variation performance.

FLC does not require any mathematical model of the controlled system. Its rules can be expressed based on a series of logical statements.

To have a constant speed of the turbine, it is necessary to maintain the pressure at the inlet of the constant turbine. This adjustment at the inlet is provided by the servo valve controlled by a PI regulator, as shown in figure 8.

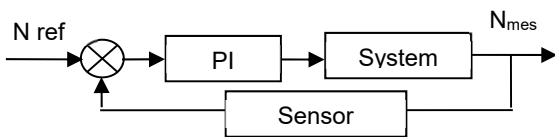


Fig.8.Closed loop with PI

The flow rate is fixed across the turbine, and a reference speed is applied to the system, controlled by two PI and AFLC regulators.

The closed-loop block represents the configuration of the turbine speed control in figure 9.

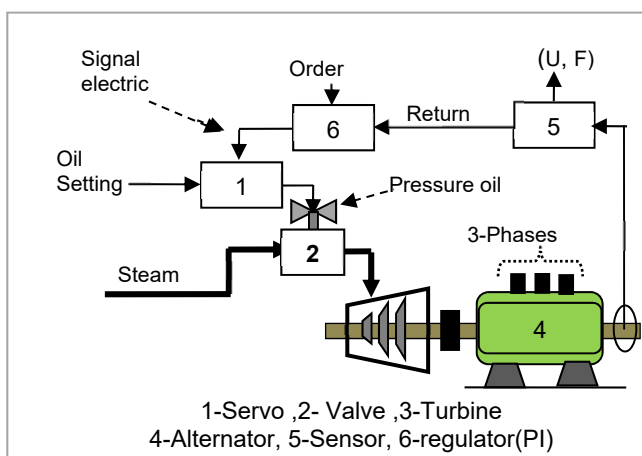


Fig. 9 Speed regulation synoptic diagram

IV.3. Turbine speed control with Adaptive Fuzzy PI Controller Type 1 (AFLC-PI).

Fuzzy logic is used to represent uncertain and imprecise knowledge. Fuzzy control is used to make decisions even if one can only estimate the inputs and outputs from vague predicates.

It can control nonlinear, uncertain, and adaptive systems, giving robust parameter variation performance.

FLC does not require any mathematical model of the controlled system. Its rules can be expressed based on a series of logical statements.

To overcome the disadvantages of PI controllers, we propose a hybrid controller, in which the parameters of the PI controller are adjusted by an adaptive mechanism based on fuzzy inference (AFLC-PI).

The proposed diagram uses fuzzy rules to determine the parameters of the PI controller that generates the control action signal, as shown in Figure10.

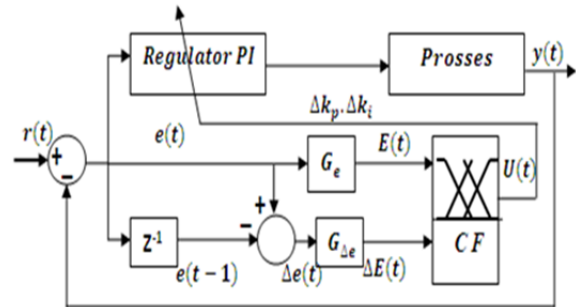


Fig.10.The adaptive type1 AFLC -PI controller

The adaptive (AFLC-PI) is designed as a supervisory controller that updates the gain values for the PI controller according to the parameter requirements of variations during operation.

In our case, we will adjust the parameters (gain) according to the error and its derived values.

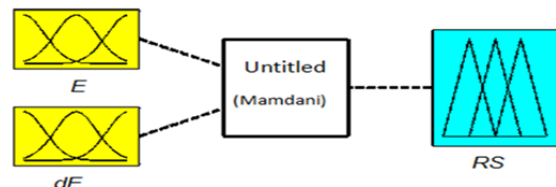


Fig.11. Fuzzy Controller Schematic Diagram

The inputs of the fuzzy supervision controller being E the error and its derivative dE / dt , while the normalized values of K_p and K_i are outputs as shown in figure 10.

Figure 12 and Figure 13 show the membership functions for the error, and they derived dE / dt , respectively.

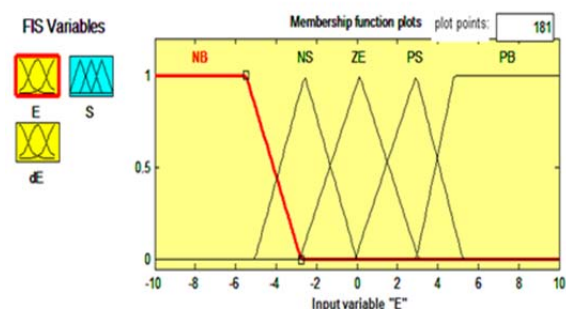


Fig.12.Membership Functions for Error E

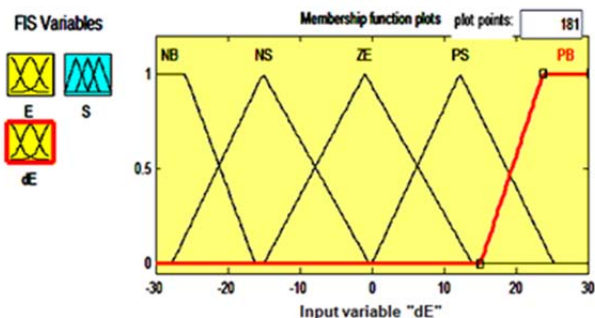


Fig. 13. Membership Functions for dE/dt .

V. Simulation and results.

Simulation is carried out to compare the turbine performance with PI and adaptive fuzzy logic speed controllers. The system presented below with different controllers is realized in Matlab/Simulink and has been simulated. The turbine reference speed was set at 3000 tr/min, and the measured turbine speed was observed for each controller.

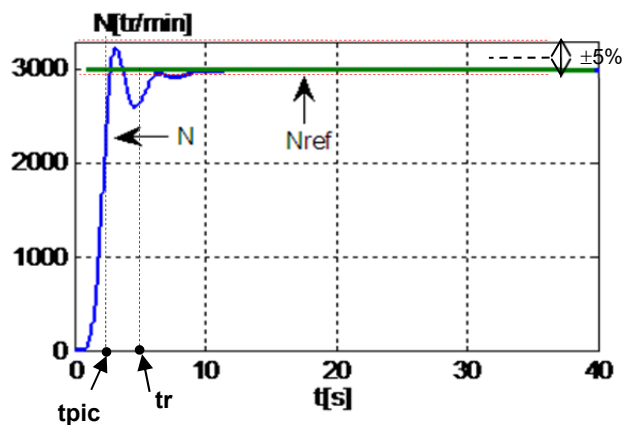


Fig. 14. Speed curve with PI controller.

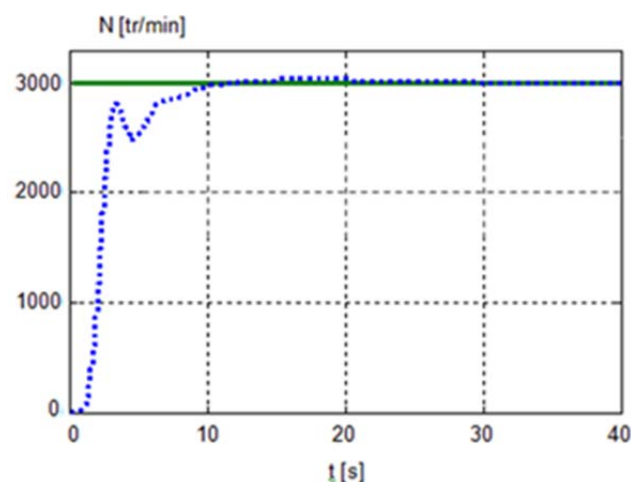


Fig. 15. Speed curve with AFLC controller

We see in figure 14 that the turbine's rotation speed follows its reference with a rapid dynamic accompanied by a tolerated overshoot. It can be concluded that the PI regulator ensures reasonable speed control with better performance.

- Response time: $tr=5.55s$
- Over shoot $D = 6.66\%$ correspent au temps critique

- $tpic = 2.96s$.
- Zero static error

Figure 15 presents the turbine speed for the adaptive fuzzy logic controller. Also, we can see clearly that the turbine speed follows its reference with a rapid dynamic, and good performance:

- Response time: $tr=?$
- Over shoot $D = ? \%$ correspent au temps critique
- $tpic = ? s$.
- Zero static error
- Comparison between the two curves.

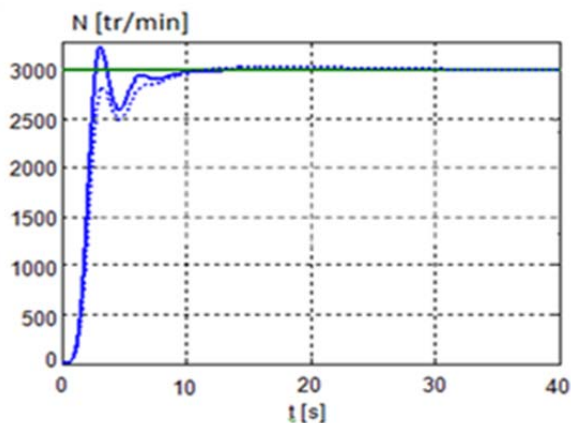


Fig. 16.Speed curve with AFLC controller

From figure 16, the results show that the rise time is almost the same with the two types of regulation.

A clear difference between the two regulators appears in the exceeding response time and static error.

The simulation results, therefore, show the superiority of the AFLC-PI adaptive controller, where the system responds and stabilizes quickly with a tolerated overtaking.

Conclusion

- The variation of the exchanger's temperature by action on various parameters such as the length, the heat exchange surface, and the heat exchange coefficient has been concluded.

- A comparison was made between conventional and advanced control for driving a steam turbine. It is noted that the response time does not differ much, while the damping with AFLC-PI adaptive is better compared to conventional control.

This research is described by the following steps:

We showed the problem of the climate and the emissions of greenhouse gases (GHG) with the numbers given by the International Climate Agency (AIC).

We clarified the responsibility of polluting countries and their use of primary energy despite having signed all the agreements with AIC.

We went directly to solar energy and specifically to a solar thermal power plant.

We were given a diagram in which I specified the main components, such as the sensor, the heat exchanger, and the turbine, and I cited an essential element in the command (servo valve).

We explained the working principle based on diagram 6.

We went through a little introduction to the PI regulator and fuzzy logic.

For the PI parameters, I used the ZIEGLER-NICHOLS method.

We applied a speed instruction (3000 tr/m).

The results were good regarding response time, overshoot, and static error.

Our perspectives in the following work are to add a single-axis solar tracking system and hybridize it with photovoltaic energy accompanied by another order.

REFERENCES

- [1] Ahmedzai S., Mckinna A., Afghanistan electrical energy and trans-boundary water systems analyses: Challenges and opportunities, *Energy Reports.*, 4 (2018), 435-469
- [2] Wang Y., Qu K., Chen X and Riffat S., Holistic electrification vs deep energy retrofits for optimal decarbonisation pathways of UK dwellings: A case study of the 1940s' British post-war masonry house, *Energy.*, 241 (2022), 122935
- [3] Energy Information Administration., World energy consumption by source and sector, *Monthly Energy Review (April 2022).*,
- [4] Ciavarella, A., Cotterill, D., Stott, P. et al., Prolonged Siberian heat of 2020 almost impossible without human influence, *Climatic Change.*, 9 (2021), No. 166
- [5] *International Energy Agency., World CO2 emissions from fuel combustion by fuel, 1971-2019, Online: <https://www.iea.org/data-and-statistics/charts/world-co2-emissions-from-fuel-combustion-by-fuel-1971-2019>., Consulted: 26/08/2022.*
- [6] Zara-Moya, E., High Efficiency Plants and Building Integrated Renewable Energy Systems, *Handbook of Energy Efficiency in Buildings.*, 2019, 441-495
- [7] Zhang, T., Wang, R., Concentrating Solar Thermal Power, *A Comprehensive Guide to Solar Energy Systems.*, 2018, 127-148
- [8] Murshitha Shajahan M. S., Najumnissa Jamal D., Mathew J and Anas Ali Akbar A., Improvement in efficiency of thermal power plant using optimization and robust controller, *Case Studies in Thermal Engineering.*, 33 (2022), 101891
- [9] Alobaid F., Mertens N., Starkloff R and Lanz T., Progress in dynamic simulation of thermal power plants, *Progress in Energy and Combustion Science.*, 59 (2017), 79-162
- [10] Al-Maliki W. A. K., Hadi A. S., Al-Khafaji H. M. H and Alobaid F., Dynamic modelling and advanced process control of power block for a parabolic through solar power plant, *Energies.*, 15 (2022), No.129, 1-20
- [11] Cao H., Wang Y and Jia L., Adaptive Neuro-Fuzzy Inference System-Based Pulverizing Capability Model for Running Time Assessment of Ball Mill Pulverizing System, *Przegląd Elektrotechniczny.*, 5 (2013), No.89, 122-127
- [12] Liao X., Liu K., Qin L., Wang N., Ma Y and Chen Z., Cooperative DMPC-Based Load Frequency Control of AC/DC Interconnected Power System with Solar Thermal Power Plant, *2018 IEEE PES Asia-Pacific Power and Energy Engineering Conference (APPEEC).*, 2018, 341-346
- [13] Terunuma R., Ohmori H., Model predictive control for concentrating solar power plants with thermal energy storage system, *2020 59th Annual Conference of the Society of Instrument and Control Engineers of Japan (SICE).*, 2020, 274-279
- [14] Chochowski A., Czekalski D and Obstawski P., Dynamic properties flat solar collectors, *Przegląd Elektrotechniczny.*, 6 (2010), 257-263
- [15] Bishoyi D., Sudhakar K., Modeling and performance simulation of 100MW PTC based solar thermal power plant in Udaipur India, *Case Studies in Thermal Engineering.*, 10 (2017), 216-226
- [16] Salgado-Conrado L., A review on sun position sensors used in solar applications, *Renewable and Sustainable Energy Reviews.*, 82 (2018), No.3, 2128-2146
- [17] Estrada-López J. J., Castillo-Atoche A. A and Sanchez-Sinencio E., Design and Fabrication of a 3-D Printed Concentrating Solar Thermoelectric Generator for Energy Harvesting Based Wireless Sensor Nodes, *IEEE Sensors Letters.*, 3 (2019), No.11, 1-4
- [18] Ni G., Li G and Boriskina S., Steam generation under one sun enabled by a floating structure with thermal concentration, *Nat Energy.*, 1 (2016), 16126
- [19] Hossain M. S., Saidur R., Fayaz H., Rahim N. A., Islam M. R., Ahamed J. U., and Rahman M. M., Review on solar water heater collector and thermal energy performance of circulating pipe, *Renewable and Sustainable Energy Reviews.*, 15 (2011), No.11, 3801-3812
- [20] Pranesh V., Velraj R., Christopher S and Kumaresan V., A 50-year review of basic and applied research in compound parabolic concentrating solar thermal collector for domestic and industrial applications, *Solar Energy.*, 187 (2019), 293-340
- [21] Hussaini Z. A., King P and Sansom C., Numerical Simulation and Design of Multi-Tower Concentrated Solar Power Fields, *Sustainability.*, 12 (2020), 1-22
- [22] Mariana S., Bretado-de L. R., Carlos I and Nigam K. D. P., An overview of sustainability of heat exchangers and solar thermal applications with nanofluids: A review, *Renewable and Sustainable Energy Reviews.*, 142 (2021), 10855
- [23] Cai X. F., Zhang X. L., Zhou P., Rahim N. A., Islam M. R., Ahamed J. U., Rahman M. M., Xu D., Cai W. J., Chen X. Y., Shao Y. X and Wang J., Governor System for 300MW Hydraulic Generator in Xiangshuijian Pumped-Storage Power Station, *Advanced Materials Research.*, 347 (2012), 525-536
- [24] Aourousseau A., Vuillerme V and Bezian J. J., Control systems for direct steam generation in linear concentrating solar power plants – A review, *Renewable and Sustainable Energy Reviews.*, 56 (2016), 611-630
- [25] Birnba J., Eck M., Hirsch T., Lehmann, D and Zimmermann G., A Direct Steam Generation Solar Power Plant with Integrated Thermal Storage, *ASME. J. Sol. Energy Eng.*, 132 (2010), No.3, 031014
- [26] Jelali M., Huang B., Detection and Diagnosis of Stiction in Control Loops, *Advances in Industrial Control.*, Springer, doi:10.1007/978-1-84882-775-2
- [27] Al Ibrahim E., Lachhab S. E., Hamdaoui F., El Amrani I., Achhar A and Dimi L., Modeling of a cylindro-parabolic solar collector and simulation by Matlab software, *International Journal of Scientific & Engineering Research.*, 8 (2017), No. 10, 1135-1139
- [28] Bougriou C., Baadache K., Shell-and-double concentric-tube heat exchangers software, *Heat Mass Transfer.*, 46 (2010), 315-322